Triplet−Triplet Energy Transfer as a Tool for Probing Molecular Diffusivity within Zeolites

Shuichi Hashimoto,*,† Masahide Hagiri,† and Alexander V. Barzykin*,‡

Chemistry Department and Advanced Engineering Courses, Gunma College of Technology, Maebashi, Gunma 371-8530, Japan, and National Institute of Advanced Industrial Science and Technology, Tsukuba, Ibaraki 305-8565, Japan

Received: September 10, 2001; In Final Form: November 5, 2001

Quenching of photoexcited triplet-state anthracene through triplet−triplet (T−T) energy transfer mechanism by a few energy acceptors, azulene, ferrocene, and also anthracene in the ground state, is investigated in a dehydrated Na^+ form of zeolite Y (NaY) with a transient absorption spectroscopy utilizing a diffuse reflectance detection technique. It is found that the decay curves of T−T absorption for anthracene follow unconventional kinetics that can be handled by a model based on the continuous time random walk (CTRW) theory. The analysis of the quenching kinetics affords an estimate of the intrazeolite self-diffusion coefficient for the guest aromatic species. Presently, a simplified version of the CTRW treatment is developed which enables us to extract information concerning the diffusivity only by analyzing the long time tail of triplet decay signals measured by a conventional photomultiplier detection system with limited time resolution. The self-diffusion coefficients thus obtained, ranging from 10^{-15} to 10^{-16} m^2 s^{-1} in NaY at 298 K, are significantly smaller than those observed for benzene (10^{-10}−10^{-13} m^2 s^{-1}). This study demonstrates that the triplet quenching method is a powerful technique for evaluating diffusion coefficients of relatively large organic molecules with small intrazeolite mobility that are hardly measurable by NMR and other traditional techniques.

Introduction

Diffusion of adsorbed molecules within the intracrystalline cage network of zeolites is important in influencing chemical reactions of the guest species and thus in determining the overall catalytic effects of the zeolite hosts.[1−4] In the usual cases, the molecules introduced externally into zeolites are not fixed at particular sites but migrate by executing a hopping motion from one adsorption site to another within the same cage and occasionally to other cages through one of the interconnecting windows. Transport properties, such as intra- and intercage mobility of benzene in NaX and NaY zeolites, have been studied with the NMR spin−lattice relaxation[5] and the pulsed field-gradient (PFG) NMR techniques.[6] Self-diffusion coefficients, their loading dependence, and activation energies of diffusion were measured. The picture of molecular diffusivity thus obtained is still in a developing stage, and there remains a discrepancy among quantitative figures derived from different methods. For instance, experimentally observed values for the self-diffusion coefficient of benzene in NaY at room-temperature range from 10^{-10} to 10^{-13} m^2 s^{-1}, depending on the source.[5−8] Recent molecular dynamics[5b,c,9] and Monte Carlo simulation techniques[5d,10] have given access to the diffusion coefficients and the activation energy of diffusion on the molecular level. These results provided a sound clue to the controversial picture, but there still remains room for experimental support.

The transport properties within zeolites correlate closely with other important molecular properties such as adsorption and spatial distribution. The distribution of the guest species among the cages is, in turn, governed by the interaction between the guest molecules themselves and between the guest molecules and the zeolitic sites responsible for adsorption. Experimental investigations focusing on the adsorption and distribution properties have also been carried out. For example, small aromatic species such as benzene were predicted to be adsorbed within the supercages of zeolites X and Y interacting primarily with the cationic sites, as revealed by a solidlike Pake pattern in ^2H NMR spectra,[5] and secondarily with the 12-membered ring window sites, as elucidated by the powder neutron diffraction.[11] As for the issue of the distribution, Xe atoms in the α cages of NaA zeolite have been investigated with the ^{129}Xe NMR chemical shift.[12] Poisson occupation statistics were suggested to be applicable to the Xe distribution at low loading levels.

Despite the ample studies carried out on the diffusivity of benzene and its analogues, little is known about the diffusion properties of aromatic molecules larger than benzene in zeolites because of the limitations inherent in measurements. For example, the PFG NMR is only applicable to the determination of the diffusion coefficients in the range from 10^{-10} to 10^{-13} m^2 s^{-1}, because of the requirement of $\Delta \ll T_2$, where Δ represents the time separation between two magnetic field gradient pulses (typically $\Delta = 1-100$ ms) and T_2 is the spin−spin relaxation time.[13] Another powerful technique for measuring diffusivity in zeolites, quasielastic neutron scattering (QENS),[7] faces difficulty in measuring slow diffusion because of the limitation of the time scale of the measurements ($10^{-12} < \tau < 10^{-8}$ s).

Here we present an alternative experimental technique, based on photochemistry, for acquiring diffusion coefficients of various aromatic species adsorbed in zeolite particles. The technique basically observes the quenching kinetics of excited probes produced by a pulsed-laser excitation. The probe molecules are

* To whom correspondence should be addressed.
† Gunma College of Technology.
‡ National Institute of Advanced Industrial Science and Technology.

10.1021/jp013461v CCC: $22.00
Published on Web 01/04/2002

expected to either self-deactivate or undergo quenching through collision with another doped species (a quencher) continuously migrating within the cage networks. Especially, an excited triplet state is appropriate for the probe, and the triplet energy acceptors are suitable for the quencher[14] because the triplet−triplet energy transfer proceeds mainly through a collisional mechanism because of exchange interaction.[15] The general method of time-resolved diffusion-mediated excited-state deactivation has already found successful application for probing dynamical and structural properties of a variety of microheterogeneous media, such as colloids.[16] More recently, we have developed a treatment that describes quenching kinetics in zeolites by applying the continuous time random walk (CTRW) model. This approach was tested experimentally and found to be applicable to the quenching of the triplet-state anthracene by azulene in dehydrated zeolite NaY; the diffusion coefficient of azulene was obtained.[17] Our triplet-quenching method has a potential to determine the diffusion coefficients for many aromatic species adsorbed within zeolites that are not measurable with the traditional techniques. It is pertinent to note that Johnston and co-workers[18] have previously investigated recombination kinetics of diphenylmethyl radicals generated in the cages of NaX zeolite both experimentally and theoretically. To model the kinetics of the diphenylmethy radicals, they assumed that the radicals perform random walks on a diamond lattice, and they explained the experimental decay curves ranging from 300 ns to 1 ms on the basis of their numerical simulations.

In the present study, we employed a conventional photomultiplier detection system for the measurement of the triplet decay signals instead of the previous pump−probe method,[17] which had a 10 ns time resolution. Although we sacrificed the time resolution, we saved time for the measurements substantially. In addition, we developed an analytical expression that simplifies the general CTRW result for the quenching kinetics of triplet probes. It is based on matching exact asymptotic expansions. The short-time behavior is shown to be analogous to the luminescence quenching decay in micelle solutions. On the other hand, the long-time behavior is described by the Smoluchowski type of kinetics. The diffusion coefficient of the guest species can be obtained by fitting an approximate decay function only to the long-time tail of the experimental curves, even though the time resolution is rather poor. By this treatment, we obtained results in good agreement with our previous pump−probe studies for the anthracene−azulene system.

Experimental Section

The experimental setup for a nanosecond diffuse reflectance laser photolysis,[19] which is applicable to the detection of transient species in optically inhomogeneous and light-scattering systems, is described briefly in the following. The third harmonics ($\lambda = 355$ nm) of a pulsed Nd:YAG laser (Continuum Surelite II-10; pulse width, 6 ns) was used as an excitation light source and a 150 W short arc Xe lamp (Hamamatsu L2274) was used as a monitor light. Optical filters consisting of a 10 cm pass-length water filter, an infrared-cutoff filter, neutral density filters, and a band-pass filter (420 nm) were employed. Time evolution of the transient absorption was monitored with a photomultimlier (Hamamatsu R928) through a monochromator (Ritsu MC-10DG; focal length, 10 cm; 1200 grooves/mm; blaze, 500 nm). A signal from the photomultiplier was fed to a digital oscilloscope (Tektronix TDS540A, 500 MHz, 1 G samples/s) that was controlled by a personal computer.

Anthracene (Fluka, scintillation grade), azulene (Tokyo Kasei), and ferrocene (Wako) were recrystallized. The sodium form of zeolite Y (NaY, Si/Al = 2.8, Na/Al = 1.0) with an average particle diameter of 5−10 μm was obtained from Tosoh. Zeolite powder was calcined in air at 500 °C for 8 h just before sample preparation. Anthracene-doped zeolite samples were prepared by adsorption from *n*-hexane solution. The dehydrated zeolite powder was stirred in *n*-hexane solution of anthracene in a stoppered vial at room temperature for 10 min; the sample was filtered, and the solid was washed twice with *n*-hexane. All of the procedures were carried out in a nitrogen-filled globebox. The samples were transferred into 2 mm thick Suprasil cells and evacuated at <0.4 Pa for 12 h and at 100 °C. The water content in the dehydrated samples is estimated to be less than 0.4 wt % with ^{1}H NMR measurements using anthracene as an internal standard. Azulene and ferrocene were adsorbed by sublimation in vacuo at room temperature into the zeolite doped with anthracene. Azulene-doped samples were kept at 80 °C for 40 h to allow the diffusion of dopants, whereas ferrocene-doped samples were kept at room temperature for more than 3 months in order to minimize thermal oxidation of ferrocene in zeolite Y.[20]

Background for Data Analysis

Kinetics of the excited-state quenching in zeolites is most conveniently described in terms of the CTRW model.[21,22] In its simplest but still quite realistic formulation it assumes that quenchers perform independent random walks which involve unbiased jumps to nearest-neighbor lattice sites, and the waiting time distribution function in each site is exponential. The lattice site is normally associated with a zeolite supercage, but generalization to true adsorption sites is possible. Supercages are assumed to be occupied by reactants at random, according to the Poisson law. The reaction is assumed to take place whenever the probe and the quencher are in the same supercage. For open zeolite structures, quenching may also occur when the probe and the quencher reside in the neighboring supercages. The final expression for the experimentally observable excited-state survival probability $\Phi(t)$ is given by[17]

$$-\ln \Phi(t) = k_0 t + \bar{n} R(t) \tag{1}$$

where k_0 is the excited-state self-decay lifetime, $\bar{n}$ is the average number of quenchers per supercage ([quencher]/[supercage], typically, $\bar{n} \ll 1$), and the time-dependent reaction flux $R(t)$ is defined in terms of its Laplace transform:

$$\hat{R}(s) = s^{-2} \langle\langle [\mathbf{W}^{-1} + \mathbf{G}(s)]^{-1} \rangle\rangle \tag{2}$$

Here $\hat{R}(s) = \int_0^\infty \mathrm{d}t\, R(t) \exp(-st)$ denotes the transform, double angular brackets imply summation of all matrix elements, $W_{\mathbf{r}\mathbf{r}'} = \delta_{\mathbf{r}\mathbf{r}'} w(\mathbf{r})$, $w(\mathbf{r})$ is the quenching rate constant from a position $\mathbf{r}$ of the quencher relative to the probe, $\delta_{\mathbf{r}\mathbf{r}'}$ is the Kronecker delta, and

$$G_{\mathbf{r}\mathbf{r}'}(s) = (s + k_\mathrm{m})^{-1} g[\mathbf{r} - \mathbf{r}', k_\mathrm{m}/(s + k_\mathrm{m})] \tag{3}$$

where $g(\mathbf{r},\xi)$ is the so-called random walk generating function and k_m is the rate constant for the intercage migration. Methods of calculating $g(\mathbf{r},\xi)$ for different lattices are known.[21]

From now on, we will focus on the diamond lattice of NaY zeolite and consider several practically useful simple approximations from the above rigorous results. Our strategy will be to derive exact asymptotic expressions for $R(t)$ in the limit of short times, $R_\mathrm{ST}(t)$, and long times, $R_\mathrm{LT}(t)$, and then match them as follows:

$$R(t) = R_{ST}(t)e^{-k_m t} + R_{LT}(t)[1 - e^{-k_m t}] \quad (4)$$

We have multiplied the first term by $\exp(-k_m t)$ in order to cut this part of solution at long times. The effect on the short-time behavior is minor. Similar arguments apply to the cutoff factor for the second term. Details of the derivation for $R_{ST}(t)$ and $R_{LT}(t)$ are given in the Appendix. Here we consider final results for two different modes of quenching.

Quenching Mode 1: Intracage Quenching. If the quenching takes place only when the probe and the quencher share the same supercage, $R_{ST}(t)$ and $R_{LT}(t)$ are given by

$$R_{ST}(t) = \frac{k_q^2}{(k_q + k_m)^2}[1 - e^{-(k_q + k_m)t}] + \frac{k_q k_m}{k_q + k_m} t \quad (5)$$

$$R_{LT}(t) = k_\infty t\left(1 + g_0 \frac{k_\infty}{k_m} \frac{2}{\sqrt{\pi k_m t}}\right) + c \quad (6)$$

where

$$k_\infty = \frac{k_q k_m}{k_m + g_0 k_q} \quad (7)$$

$k_q = w(0)$ is the pseudo-first-order rate constant for the intracage quenching, and c and $g_0 = 1.79288$ are constants associated with the lattice structure.

It should be noted that eq 5 has exactly the same form as that derived for luminescence quenching in micelle solutions.[23] It is easy to understand, because at short times the reactants do not have a memory of the zeolite structure. On the other hand, in micelles, the migration occurs via the bulk aqueous phase where mixing is effectively infinitely fast, and thus, there is no memory of the solution structure at all times.

Equation 6 predicts the same type of behavior as it follows from the Smoluchowski equation for the diffusion-controlled reactions.[24] This is quite understandable because diffusion is a continuous limit of the discrete random walk. By comparing eqs 5 and 6, we can see the difference in their predictions for the long-time rate constant k_∞ − a factor of g_0 in the denominator. It is this factor that reflects the memory of the lattice structure. The difference is maximal when $k_q \gg k_m$, where we have $k_\infty = k_m/g_0$.

k_q and k_m are adjustable parameters for fitting the experimental decay curves. In principle, c can be calculated analytically in terms of k_q and k_m, but the results are cumbersome (particularly when intercage quenching is involved, as discussed in the next subsection). So we took c as the third fitting parameter. We do not need its value, but we need it to be there in the fitting procedure. The reason we need c at all is because the diamond lattice has a very low coordination number of four and is thus explored by quenchers very slowly. We found that under our experimental conditions we need to keep three terms in the series expansion of $R(t)$ in order to reproduce the long-time behavior correctly.

As a test of the above approximate solution, we performed the following numerical experiment: generated the exact data for $k_q = 5$ and $k_m = 1$, added 5% of white noise to the survival probability, and then extracted back k_q and k_m by fitting the resulting data using eqs 4−7. The parameters obtained from the fit are $k_q = 5.17$ and $k_m = 1.009$.

Quenching Mode 2: Intracage plus Intercage Quenching. We have previously encountered the situation where the observed quenching is much more efficient than one would expect solely on the basis of the intracage quenching mechanism.[17] In this case, the reaction takes place not only when the probe and the quencher share the same supercage but also when they are located in the neighboring cages (four cages of the first coordination sphere). This quenching mechanism reflects an open structure of the zeolite framework: the windows connecting the cages are so wide-open that the reactants can closely approach each other even if they reside in different (neighboring) cages. Here, complementary to the rate constant k_q for quenching in the same supercage, one can introduce the rate constant $k_q' = w(1)$ for quenching from the neighboring supercage. The latter process is most likely governed by the intracage hopping, which is typically much faster than the intercage migration. Thus, we expect generally that $k_q > k_q' > k_m$. It is also reasonable to expect that $k_q \gg k_q' > k_m$ because typically the size of the system is such that once the probe and the quencher are within the same supercage they are actually in contact and react immediately. This is what we have assumed in deriving the following approximate formulas for $R_{ST}(t)$ and $R_{LT}(t)$ (see the Appendix for details):

$$R_{ST}(t) = (1 - e^{-k_q^{eff} t}) + 4\left(\frac{k_q^{eff}}{k_q^{eff} + k_m^{eff}}\right)^2 [1 - e^{-(k_q^{eff} + k_m^{eff})t}] + 4\frac{k_q^{eff} k_m^{eff} t}{k_q^{eff} + k_m^{eff}} \quad (8)$$

$$R_{LT}(t) = k_\infty t\left(1 + g_0 \frac{k_\infty}{k_m} \frac{2}{\sqrt{\pi k_m t}}\right) + c \quad (9)$$

where

$$k_q^{eff} = k_q' + \frac{1}{4}k_m \quad (10)$$

$$k_m^{eff} = \frac{3}{4}k_m \quad (11)$$

$$k_\infty = \frac{4k_q^{eff} k_m^{eff}}{3(g_0 - 1)k_q^{eff} + k_m^{eff}} \quad (12)$$

We can see that the structure of the obtained short- and long-time expressions is basically the same as before. The first term on the right-hand side of eq 8 corresponds to rapid quenching of those probes which happened to be in the same supercage with a quencher at time zero. The second term represents the micelle-like kinetics because of quenching from the four supercages of the first coordination sphere with the average of $4\bar{n}$, the effective quenching rate constant k_q^{eff}, and the effective migration rate constant k_m^{eff}. The meaning of the effective rate constants becomes clear after realizing that a quencher residing in the supercage neighboring to the probe has a $^1/_4$ chance to jump into the cage with the probe and a $^3/_4$ chance to jump into a cage without the probe. Equation 9 shows that the long-time behavior is universal in terms of k_∞. The memory of the structure is accumulated in the factor of $3(g_0 - 1) \simeq 2.3786$. If $k_q' \gg k_m$, then $k_\infty = k_m/(g_0 - 1)$.

As a test of the above approximate solution, we performed the following numerical experiment: generated the exact data for $k_q' = 3$ and $k_m = 1$ (assuming that $k_q \gg k_q', k_m$), added 5% of white noise to the survival probability, and then extracted back k'_q and k_m by fitting the resulting data using eqs 4 and 8−12

(discarding the first term in eq 8). The parameters obtained from the fit are $k'_q = 2.8$ and $k_m = 1.015$.

To determine the rate constants for quenching, it is crucial to observe the initial rapid stage of the decay. However, because the main goal of our studies is the migration rate (or, equivalently, the diffusion coefficient), we can sacrifice the resolution of the experimental setup and gain certain advantage by looking only at the long-time behavior. At long times, we can use eq 9 for fitting and choose k_∞, k_m, and c as adjustable parameters. As we have seen, the long-time behavior is universal for any quenching mechanism. Let us do the following numerical experiment: generate the decay with $k_q = 100$, $k'_q = 10$, and $k_m = 1$ and add white noise, then shift the origin of the coordinate system as if we do not see the initial stage, and finally try to fit the observed decay by eq 9. We obtain $k_\infty = 1.27$ and $k_m = 1.12$. Basically, not bad for k_m. However, if we knew the quenching mechanism, the accuracy would be higher. Let us explain this point. Because now we are in the limit that both quenching rates are much larger than the migration rate, then k_∞ should be either k_m/g_0 for *mode 1* or $k_m/(g_0 - 1)$ for *mode 2*; that is, in the former case, k_∞ should be smaller than k_m, whereas in the latter case, it should be larger. We observe in our numerical experiment that $k_\infty > k_m$. Thus, we can assume the intercage quenching mechanism (as it actually is in our input). If we calculate k_m from $k_\infty = k_m/(g_0 - 1)$ taking k_∞ from the fitting, we obtain $k_m = 1.007$.

In concluding this section, we should also note that it follows from eq 1 that the function

$$F(t) = -R(t) = \frac{1}{\bar{n}}[\ln \Phi(t) + k_0 t] \qquad (13)$$

must be universal for any quencher concentration, as long as low quencher concentrations are employed ($\bar{n} \ll 1$). $F(t)$ can be thought of as the decay function in the presence of just one quencher and in the absence of self-deactivation. Equation 13 was used as a test of applicability of the present treatment to the experiments.

Results and Discussion

1. Anthracene Triplet Quenching in Dehydrated NaY: Intracage and Intercage Quenching. Anthracene was chosen as a probe molecule because of its large extinction coefficient of triplet−triplet absorption together with its markedly long triplet lifetime. A large extinction coefficient is preferable to fulfill the experimental condition, [probe*] ≪ [quencher], whereas a long lifetime of an excited probe is essential for the observation of quenching by a slowly diffusing quencher within the zeolite cage network. The ϵ value of 64 700 M^{-1} cm^{-1} at 422.5 nm has been determined for triplet-state anthracene in cyclohexane solution.[25] Also, the decay constants of 49 ± 12 s^{-1} in benzene and 66 ± 14 s^{-1} in cyclohexane at 296 K were reported in the literature,[26] whereas somewhat smaller decay constants, between 30 and 40 s^{-1}, were measured[27] in solid media, such as poly(methyl methacrylate) (PMMA) and polystyrene (PS) at room temperature. This fact suggests that the events of impurity quenching and T−T annihilation can be minimized in solid media. An important precaution necessary for the experiment in the zeolite system is to employ a sufficiently attenuated intensity of the monitor light beam with neutral density filters in addition to the reduced excitation laser intensity. We found that the decay rate of the anthracene triplet (^{3}A*) signal at a fixed loading level of 5.0 × 10^{-6} mol g^{-1} is slower for lower intensity of the monitor light. This could be a sort of heating effect by the monitor light, because no accelerating effect was found for a pulsed monitor light (<50 μs) by which a decay constant of 60 ± 5 s^{-1} was measured. Therefore, the monitor light intensity was reduced to give the self-decay constant of 54 ± 5 s^{-1} for the triplet state anthracene at the loading level of 5.0 × 10^{-6} mol g^{-1} ($\bar{n} = 0.0079$).

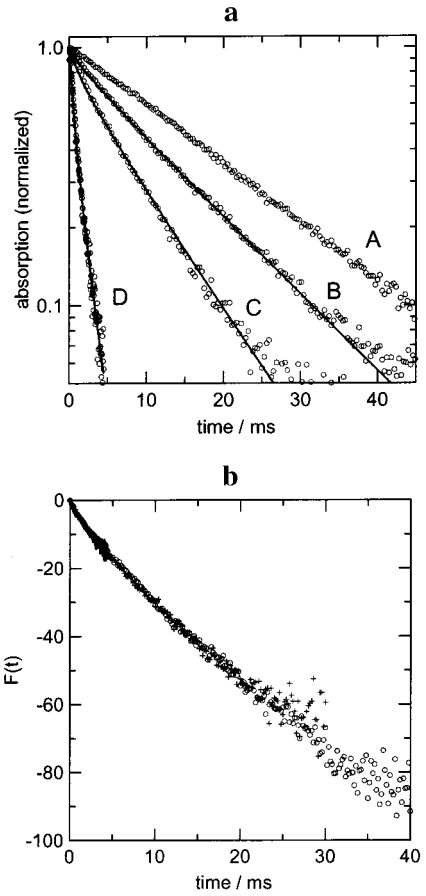

Figure 1. (a) Triplet−triplet absorption decay of anthracene in dehydrated NaY zeolite excited at 355 nm and monitored at 420 nm, at various loading levels: (A) 5.0 × 10^{-6}, (B) 1.0 × 10^{-5}, (C) 2.0 × 10^{-5}, and (D) 1.1 × 10^{-4} mol g^{-1}. The ordinate represents the normalized absorption measured by the diffuse-reflectance mode. The absorption is defined by $\Delta I/I_0$ (I_0 is the reflectance intensity before laser excitation and ΔI is the change in the reflectance after excitation), which is proportional to the concentration.[19] The values of $\Delta I/I_0$ at $t = 0$ are always less than 10%. (b) Universal plots for the experimental decay curves presented in Figure 1a. $F(t)$ is defined by eq 13 in the text. The mean occupancy numbers are (○) $\bar{n} = 0.016$, (+) 0.032, and (−) 0.18. The self-decay rate constant is $k_0 = 35$ s^{-1}.

The decay rate of the ^{3}A* signal probed at 420 nm in dehydrated NaY zeolite increases with increasing loading level. Typical experimental results are shown in Figure 1a. This finding is ascribed to self-quenching, i.e., triplet quenching by anthracene in the ground state, by analogy with a similar observation in solution.[26,28] The decay curve obtained at a low loading level of 5.0 × 10^{-6} mol g^{-1} ($\bar{n} = 0.0079$) was approximated by a single-exponential function, whereas the nonexponential nature was obviously noted at higher loadings. Universality of the decays was checked according to eq 13 as illustrated in Figure 1b. For this plot, the choice of the value of k_0 is critical. Making use of the observed value of ca. 50 s^{-1} for k_0 was unsatisfactory. Instead, 35 s^{-1} was used in Figure 1b. The reason for this can be that the experimentally observed k_0 is still affected by the monitor light or suffers impurity quenching because the values of k_0 ranging from 30 to 40 s^{-1} have been reported[27] in the solid media at room temperature,

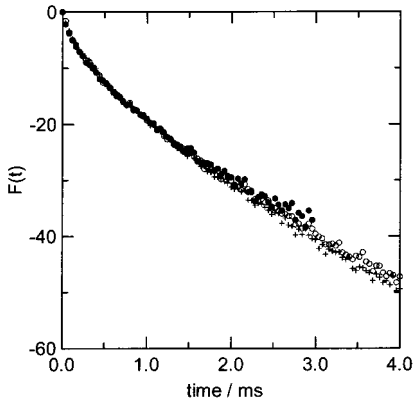

Figure 2. Universal plots for the quenching of triplet state anthracene by azulene in dehydrated NaY. The loading level of anthracene is 5.0 $\times$ 10^{-6} mol g^{-1}, and the mean occupancy numbers of azulene are (○) $\bar{n} = 0.012$, (+) 0.029, and (●) 0.047. The self-decay rate constant is $k_0 = 50$ s^{-1}.

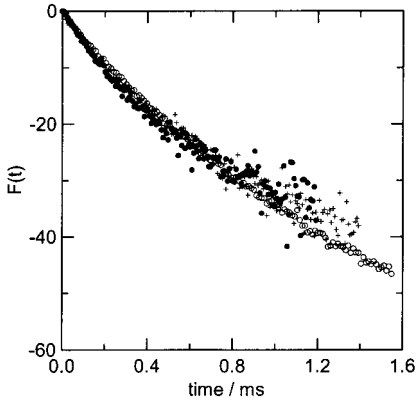

Figure 3. Universal plots for the quenching of triplet state anthracene by ferrocene in dehydrated NaY. The loading level of anthracene is 1.0 $\times$ 10^{-5} mol g^{-1}, and the mean occupancy numbers of azulene are (○) $\bar{n} = 0.038$, (+) 0.052, and (●) 0.087. The self-decay rate constant is $k_0 = 50$ s^{-1}.

as mentioned. Experimentally observed universality suggests that the CTRW model is applicable to the self-quenching of ^{3}A*.

Before proceeding to the analysis of the quenching data, let us first consider quenching of ^{3}A* by other quenchers, i.e., azulene and ferrocene, also in dehydrated NaY. The triplet energy level[29] of each molecule has been determined to be 14 870 cm^{-1} for anthracene, 13 600 cm^{-1} for azulene, and 13 300 cm^{-1} for ferrocene. Thus, in principle, the T−T energy transfer from ^{3}A* to azulene or ferrocene is possible. It was indeed reported that ^{3}A* is quenched both by azulene and ferrocene in solution with a diffusion-controlled rate constant.[30] Quenching by azulene and ferrocene was actually observed in dehydrated NaY (the experimental decay curves of ^{3}A* at various loading levels of the quenchers are given in the Supporting Information). However, a certain precaution was necessary for carrying out the experiments with these quenchers. Experimental conditions similar to those for the ^{3}A* self-quenching gave an appreciably faster decay of the triplet signal relative to that observed with the pump−probe method, where a pulsed monitor light was employed. This problem, presumably caused by too wide a spectrum of the monitor light the portion of which can be absorbed by the quenchers, was avoided by the use of a band-pass filter for the monitor light beam at the monitoring wavelength of 420 nm. Figures 2b and 3b depict the universal plots, confirming the applicability of the CTRW model to the quenching kinetics. Here, the choice of the value of k_0 is not critical because the decays are very fast in the presence of the quenchers compared to the self-decay.

For the interpretation of the quenching kinetics of triplet state anthracene in dehydrated NaY, mode 2, i.e., intra- plus intercage quenching mechanism, was applied. The open cage network structure, which facilitates the intercage quenching action by the quenchers residing in the direct neighboring cages, is presumably responsible for this mechanism. Our previous pump−probe studies of ^{3}A* quenching by azulene in NaY suggested this mechanism, because the analysis of the experimental decay curves on the basis of the intracage quenching mechanism, similar to mode 1 but with $\bar{n}$ being an adjustable parameter, provided unfavorably large values of $\bar{n}$. The apparent value of $\bar{n}$ was found to be ca. five times larger than the actual value determined from the loading level of azulene. For the present experimental data, measured with the PM detection system, we found it difficult to distinguish the quenching mechanism unambiguously by scrutinizing experimental decay curves, of which the initial part is lost because of poor time resolution. Nevertheless, the obtained value of k_m is not much altered irrespective of the mechanism considered, as mentioned in the preceding section. Although it is desirable to measure the decays at higher quencher concentrations for accurate determination of the quenching mechanism (mode 1 or 2), the high concentrations of quenchers are in most cases unfavorable, because the quenchers may absorb the excitation light which will lead to poor triplet signals of the probe molecule. Also, the CTRW treatment as presented is applicable only in the low concentration limit. Thus, we used relatively low quencher concentrations of $\bar{n} \ll 1$ in the present study.

TABLE 1: Quenching Parameters and Diffusion Coefficients Obtained from the Analysis of the Experimental Decay Curves Using Simplified Analytical Expressions Based on the CTRW Model

quencher	k_q/s^{-1}	k'_q/s^{-1}	k_m/s^{-1}	$D_m/m^2\ s^{-1}$	$D_s/m^2\ s^{-1}$
azulene	∞	1.8×10^4	1.1×10^4	2.2×10^{-15}	2.1×10^{-15}
ferrocene	∞	∞	2.5×10^4	4.9×10^{-15}	4.8×10^{-15}
anthracene	∞	∞	1.7×10^3	3.0×10^{-16}	1.5×10^{-16}
anthracene[a]	∞	∞	8.2×10^2	1.7×10^{-16}	8.5×10^{-17}

[a] In 0.26 $cm^3\ g^{-1}$ hydrated NaY zeolite.

The quenching parameters obtained from fitting the experimental decay curves in terms of eqs 1, 4, and 8−12 are listed in Table 1. Although the values for k_m were unequivocally determined, we see infinite values for both k_q and k'_q, or for k_q. This is obviously due to the limitation of the experimental time resolution inherent in the present PM detection system,[31] because the pump−probe method previously showed the presence of a drop in intensity at the very early stage of the triplet decay. However, it is important to note that the value of k_m will do for our purpose, because it is k_m (inverse of the mean cage residence time, τ) which is directly related to the diffusion coefficient, D, according to the Einstein relation for the three-dimensional lattice (in the present case, the diamond lattice):[10a]

$$D = \frac{a^2}{6\tau} = \frac{k_m a^2}{6} \tag{14}$$

where a denotes the jump distance. Our previous pump−probe experiments with higher time resolution of ^{3}A* quenching by azulene in dehydrated NaY provided the following parameters: $k_q = (4 \pm 2) \times 10^5$ s^{-1}, $k'_q = (2.3 \pm 1.3) \times 10^4$ s^{-1}, and $k_m = (1.1 \pm 0.2) \times 10^4$ s^{-1}, on the basis of the rigorous CTRW

treatment.[17] The agreement of the value of k_m obtained by two different methods is satisfactory, suggesting the reliability of the present conventional experiment with simplified theoretical treatment.

We have estimated the diffusion coefficients in terms of eq 14. We assumed that a in eq 14 represents the cage-to-cage distance of 1.1 nm that corresponds to the distance between the centers of the adjacent supercages.[11] It was initially assumed in the model that the probe molecules are fixed and only the quenchers are moving. However, it is more general to consider that both species are mobile. Thus, the value of D obtained from eq 14 is actually the mutual diffusion coefficient, D_m, and the self-diffusion coefficient, D_s, is obtained from $D_m = D_s(\text{probe}) + D_s(\text{quencher})$. Both values of D_m and D_s are given in Table 1.

2. Quenching in Hydrated NaY: Intracage Quenching. Hydration of zeolites brings about remarkable changes in the mobility of incorporated guest aromatic species, as we[32] and others[33] have reported previously on the basis of the observation of triplet decay rates in the presence of various quantities of coadsorbed solvents. Most strikingly, water molecules enhance the mobility by releasing the guest aromatics from the adsorption sites when only a small quantity (0.06−0.08 $cm^3\ g^{-1}$) is present. On the other hand, a large quantity of water (0.2−0.3 $cm^3\ g^{-1}$) can reduce the mobility of the guest species by interfering with the diffusional motion (e.g., by blocking the interconnecting windows between the cages). Thus, the quenching kinetics in hydrated zeolite represents another prototype discussed in the theory section: mode 1, i.e., the intracage quenching case. An example is the self-quenching of $^3A^*$ in NaY in the presence of 0.26 $cm^3\ g^{-1}$ of water. Figure 4a shows the decay signals of the triplet-state anthracene at various loading levels. At a low loading level of 1.0×10^{-6} mol g^{-1} ($\bar{n} = 0.0016$), a nearly single-exponential decay with a decay constant of 3.1×10^2 s^{-1}, a value which is an order of magnitude larger than that in dehydrated NaY, was observed. It is not clear at this moment whether this is a limiting value similar to that at infinite dilution or a smaller decay constant could be observed at lower loadings because the experiment with further diluted samples is not possible. As expected, the faster decay was observed with increasing loading levels of anthracene, confirming the self-quenching. Note that the decay curves are totally different from those observed in the dehydrated zeolite. The universal plots for the decays with varied $\bar{n}$ superimpose quite well, except for a small deviation observed at long times (see Figure 4b).

The analysis of the decay curves was carried out according to mode 1 (eqs 1 and 4−7). Application of mode 2 to the experimental decay curves gave an irrational result: the estimated values of k_q' were larger than those of k_q. Thus, we can discard the possibility of the latter quenching mechanism. The quenching parameters and the diffusion coefficients are included in Table 1. Although we obtained very small D_s for anthracene in 0.26 $cm^3\ g^{-1}$ hydrated NaY, we should point out that the value of D_s is highly dependent on the hydration level of the zeolite.

3. Diffusion Coefficient in Zeolite NaY. Previously, the diffusion of various guest species adsorbed in zeolites was investigated by a variety of experimental techniques, as briefly mentioned in the Introduction. In particular, the simplest aromatic molecule, benzene, has been a subject of close scrutiny because of its well-characterized adsorption behavior. However, the meaning of diffusion was highly dependent on the experimental methods and conditions (guest loading, temperature, particle size, etc.). For instance, only local motion between the adsorption sites within a cage (intracage motion) was monitored with the ^2H NMR spin−lattice relaxation measurements[5] at room temperature, whereas intracrystalline or intercage diffusive motion of the adsorbed species was detected by the PFG NMR technique.[6] The diffusion coefficient of benzene in NaX and NaY at room temperature observed by the QENS experiment[7b] may also correspond to that of the intracage motion, because the root-mean-squared jump length on the time scale of this experiment (<0.6 nm) was significantly shorter than the distance between the centers of two adjacent cages (1.1 nm). Inevitably, different values have been obtained for the diffusion coefficient and the activation energy of diffusion. It is important to note that the diffusion coefficients obtained by the present triplet quenching method signify the cage-to-cage diffusivity. The time scale of the experiment is such that the zeolite structure is well explored. For example, in 4 ms (see Figure 2), azulene with the self-diffusion coefficient of 2.1×10^{-15} $m^2\ s^{-1}$ will travel approximately 7 times the cage-to-cage distance from its original position, as estimated from the corresponding root-mean-squared displacement.

Only a few studies have been carried out so far on the intrazeolite diffusivity of aromatics larger than benzene. For example, the diffusion coefficient of naphthalene in NaX and

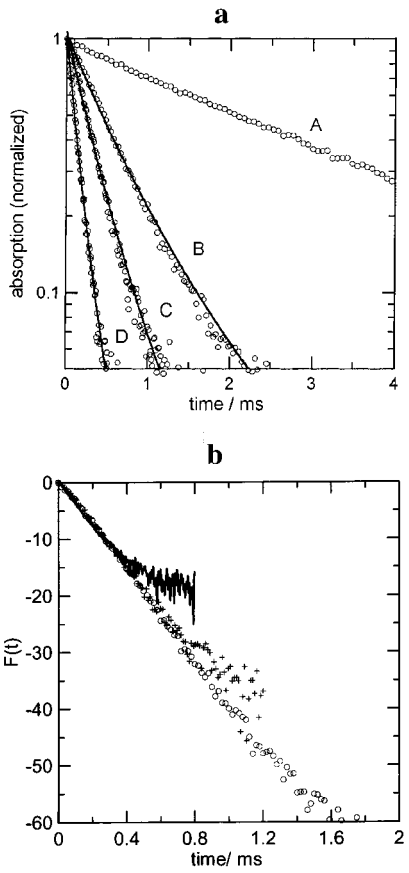

Figure 4. (a) Triplet−triplet absorption decay of anthracene in 0.26 $cm^3\ g^{-1}$ hydrated NaY zeolite excited at 355 nm and monitored at 420 nm, at various loading levels: (A) 1.0×10^{-6}, (B) 2.0×10^{-5}, (C) 4.5×10^{-5}, and (D) 1.1×10^{-4} mol g^{-1}. The values of absorption ($\Delta I/I_0$ in which I_0 is the reflectance intensity before laser excitation and ΔI is the change in the reflectance after excitation) at $t = 0$ were less than 10% and normalized in the figure. (b) Universal plots for the experimental decay curves presented in Figure 4a. $F(t)$ is defined by eq 13 in the text. The mean occupancy numbers are (○) $\bar{n} = 0.032$, (+) 0.071, and (−) 0.18. The self-decay rate constant is $k_0 = 310\ s^{-1}$, which corresponds to the decay constant for the curve A in Figure 4a.

NaY below 350 K was reported[34] to be $\sim 10^{-16}$ m^2 s^{-1}, on the basis of the measured NMR T_1 and T_2 relaxation times. A similar value of D_s for dimethylnaphthalene in NaX at 448 K was obtained with the gravimetric and chromatographic measurements.[35] Nevertheless, it is noteworthy that the self-diffusion coefficient for naphthalene represents that of the intracage motion, whereas D_s for dimethylnaphthalene is the diffusion coefficient of the intercage migration. The presently obtained values of D_s for azulene, ferrocene, and anthracene, ranging from 10^{-15} to 10^{-16} m^2 s^{-1} in dehydrated NaY, are sufficiently smaller than the literature value of the self-diffusion coefficient of benzene (10^{-10}−10^{-13} m^2 s^{-1}). It is highly possible that the diffusivity of the guest species is dependent on molecular size because of constraints on their diffusive motion imposed by the windows and walls of the zeolite. It was also pointed out that the intercage hopping dynamics of benzene is largely affected by the adsorption interaction with the host zeolite: the self-diffusion coefficient as small as 10^{-18}−10^{-19} m^2 s^{-1} was measured even for benzene in CaY, in which benzene is strongly held.[36] Thus, it is important to obtain the activation energy of diffusion in order to get an idea about the validity of the estimated D_s. The measurement of the activation energies will be conduced soon for the molecules studied presently.

Previous experiments mostly employed loadings larger than one guest molecule per supercage. On the contrary, the present method used the low loading level of much less than one guest molecule per supercage. Thus, our diffusion coefficients correspond to those free from any mutual interaction between the guest species, and care should be taken when comparing our results with the data obtained by other methods.

4. Nonexponential Quenching Kinetics. Our experimental results, and the results of others on similar systems,[33] clearly indicate that the triplet quenching kinetics in zeolites is not exponential, in contrast to normal solutions. The main reason for the observed nonexponentiality is slow diffusion. The Smoluchowski limit for the diffusion-controlled reaction rate constant, achieved quite rapidly in solutions, is not achieved at all in zeolites on the experimental time scale. Space exploration is slow because of slow diffusion and also because the coordination number of the diamond lattice is low. As a result, the diffusion-controlled reaction of triplet quenching proceeds nonexponentially (the exponential stage is not yet reached).

Nonexponential kinetics of reactions in solids are often interpreted in terms of nonhomogeneity of the adsorption sites, which gives rise to a distribution of activation energies and, hence, the distribution of rate constants. The overall kinetics is obtained by averaging the microscopic exponential decay over the above distribution (usually assumed to be Gaussian).[3] It should be noted that this procedure is legitimate only for the first-order rate processes (static reactions). Diffusion involves multiple passage over different barriers, and correct averaging should be performed over trajectories. CTRW can deal with this problem in its non-Markovian version,[21] where the waiting time distribution is defined as an average of the exponential first-order escape kinetics over the underlying distribution of activation energies. A non-Markovian expression for the reaction kinetics in zeolites is available,[17] but so far, we have not found sufficient experimental evidence that it should be used. First of all, the self-decay kinetics we observed are well described by a single exponential, indicating that adsorption sites are energetically quite homogeneous. Second, molecular dynamics simulations on benzene diffusion in NaY and NaX provide well-defined activation energies for both intra- and intercage hopping.[5] Thus, we expect also that for each of the aromatic compounds used in this study the cage-to-cage migration rate can be assigned a single compound-specific average activation energy.

Summary

We have applied a transient absorption technique utilizing a diffuse reflectance detection method in a study of triplet quenching of aromatic compounds adsorbed in NaY zeolite, aiming at the investigation of the transport properties of these molecules within zeolites. In the present study, a photomultiplier detection system was developed that can measure the time-dependent triplet decay signals at a fixed wavelength more conventionally than the previous pump−probe method. Although we sacrificed time resolution of the measurement, theoretical analysis showed that it is not a major drawback because only the long-time tail of the triplet decay signal is significant for extracting the cage-to-cage migration rate constant, which is necessary for the evaluation of the diffusion coefficient. We obtained the self-diffusion coefficients of anthracene, azulene, and ferrocene in dehydrated NaY. Such small values, ranging from 10^{-16} to 10^{-15} m^2 s^{-1} at room temperature, cannot be measured by traditional techniques, i.e., PFG NMR, and QENS. Thus, our triplet quenching method that probes longer time scales (from nanoseconds to hundreds of milliseconds) can be complementary to other established techniques.

Acknowledgment. Financial supports by Iketani Science and Technology Foundation (Grant No. 011023-A) and Izumi Science and Technology Foundation (Grant No. H13-J-62) are gratefully acknowledged.

Appendix

In the case of intracage quenching, where the reaction takes place only when the probe and the quencher share the same cage, $R(t)$ is defined in scalar form as follows:[22b]

$$\hat{R}(s) = \frac{1}{s^2}\frac{k_q(s+k_m)}{s+k_m+k_q g[0,k_m/(s+k_m)]} \tag{A1}$$

The generating function for the occupancy of the starting site $g(0,\xi)$ of a diamond lattice is given by[17]

$$g(0,\xi) = A(\xi)\left\{\frac{2}{\pi}K[B(\xi)]\right\}^2 \tag{A2}$$

where $K(x)$ denotes the elliptic integral and

$$A(\xi) = (4-\xi^2)^{1/2} - (1-\xi^2)^{1/2} \tag{A3}$$

$$B(\xi) = \frac{1}{2} - \frac{1}{4}[\xi^2(4-\xi^2)^{1/2} + (2-\xi^2)(1-\xi^2)^{1/2}] \tag{A4}$$

Let us consider the short-time expansion of the generating function by taking the $s \to \infty$ limit. In this case, we have $g[0,k_m/(s+k_m)] = 1 + {}^1/_4(k_m/s)^2 + o(s^{-3})$ and thus

$$\hat{R}(s) = \frac{1}{s^2}\frac{k_q(s+k_m)}{s+k_m+k_q} \tag{A5}$$

By inverting the Laplace transform, we obtain eq 5 of the main text. It is clear from eq 5 that the decay starts as $R(t) = k_q t$, or $-\ln \Phi(t) = k_0 t + \bar{n}k_q t$, independent of the migration rate constant. If $k_q \gg k_m$

$$R_{ST}(t) = 1 - e^{-k_q t} + k_m t \; (t \to 0) \tag{A6}$$

Now let us consider the long-time ($s \to 0$) expansion of the generating function. We have $g[0,k_m/(s + k_m)] \simeq 1.792\,88 - 1.800\,63(s/k_m)^{1/2} + 1.64736(s/k_m)$. Here we prefer to keep numbers instead of complicated analytic expressions. Finally, we are led to eq 6 of the main text. Note that the true exponential long-time behavior of the survival probability is achieved at very long times, $k_m t \gg 1$. It may not be reached in the experiment.

In the case of intra- plus intercage quenching, where the reaction takes place not only when the probe and the quencher share the same cage but also when they are located in the neighboring cages, the analysis is quite similar. **W** and **G**(s) in eq 2 are now 5×5 matrices, because five cages are involved, one central cage with the probe and four cages of the first coordination sphere of the diamond lattice. We need the generating function $g(0,\xi)$ for the occupancy of the starting site, $g(1,\xi)$ for the displacement to the nearest neighbor, and $g(2,\xi)$ for the displacement to the next-nearest neighbor (from one site of the first coordination sphere to the other via the central site). $g(0,\xi)$ is given by eq A2, and the other functions can be expressed in terms of $g(0,\xi)$ as follows:[17]

$$g(1,\xi) = \xi^{-1}[g(0,\xi) - 1] \tag{A7}$$

$$g(2,\xi) = \frac{1}{3}(4\xi^{-2} - 1)g(0,\xi) - \frac{4}{3}\xi^{-2} \tag{A8}$$

Let us first consider the short-time limit with respect to k_m^{-1}. We can write for **G**(s)

$$\mathbf{G}(s) \approx s^{-1}[\mathbf{I} - (k_m/s)\mathbf{X}] \tag{A9}$$

where **I** is the identity matrix and **X** is given by

$$\mathbf{X} = \begin{pmatrix} 1 & -1/4 & -1/4 & -1/4 & -1/4 \\ -1/4 & 1 & 0 & 0 & 0 \\ -1/4 & 0 & 1 & 0 & 0 \\ -1/4 & 0 & 0 & 1 & 0 \\ -1/4 & 0 & 0 & 0 & 1 \end{pmatrix} \tag{A10}$$

By performing matrix transformations and then summing over all elements, we obtain

$$\hat{R}(s) = \frac{k_q}{s(s + k_q)} + \frac{4k_q'}{s(s + k_q')} + \frac{k_m}{s^2}\left[\frac{k_q^{\,2}}{(s + k_q)^2} + \frac{4k_q'^2}{(s + k_q')^2} - \frac{2k_q k_q'}{(s + k_q)(s + k_q')}\right] \tag{A11}$$

We keep k_q only in the first term and assume that it is very large in the rest of the terms. Then, we rearrange eq A11 as follows:

$$\hat{R}(s) \simeq \frac{k_q}{s(s + k_q)} + \frac{4k_q^{\text{eff}}(s + k_m^{\text{eff}})}{s^2(s + k_q^{\text{eff}} + k_m^{\text{eff}})} \tag{A12}$$

where the effective rate constants k_q^{eff} and k_m^{eff} are defined by eqs 10 and 11. Inverse Laplace transformation brings us to eq 8. Quite often it happens that the intracage quenching is too fast to be seen, as discussed in the main text. Then we have

$$R_{ST}(t) = 4\left(\frac{k_q^{\text{eff}}}{k_q^{\text{eff}} + k_m^{\text{eff}}}\right)^2 [1 - e^{-(k_q^{\text{eff}} + k_m^{\text{eff}})t}] + 4\frac{k_q^{\text{eff}} k_m^{\text{eff}} t}{k_q^{\text{eff}} + k_m^{\text{eff}}} \quad (t \to 0) \tag{A13}$$

Now let us consider the long-time limit. We have already discussed the behavior of the generating function $g[0,k_m/(s + k_m)]$ for small s. Using eqs A2, A7, and A8 we obtain the expansion for the matrix **G**(s)

$$\mathbf{G}(s) \simeq \mathbf{G}(0) - g_0 k_m^{-1}\sqrt{s/k_m}\,\mathbf{1} \tag{A14}$$

where $g_0 = 1.792\,88$, as before, **1** is the unit matrix (with all elements equal to 1), and

$$k_m\mathbf{G}(0) = g_0\mathbf{1} - \begin{pmatrix} 0 & 1 & 1 & 1 & 1 \\ 1 & 0 & 4/3 & 4/3 & 4/3 \\ 1 & 4/3 & 0 & 4/3 & 4/3 \\ 1 & 4/3 & 4/3 & 0 & 4/3 \\ 1 & 4/3 & 4/3 & 4/3 & 0 \end{pmatrix} \tag{A15}$$

By performing matrix transformations and summing over all elements, we are led to eq 6 but with a different long-time rate constant:

$$k_\infty = \langle\langle[\mathbf{W}^{-1} + \mathbf{G}(0)]^{-1}\rangle\rangle \tag{A16}$$

The symmetry of **G**(0) allows us to calculate k_∞ easily. Assuming once again that $k_q \gg k_q'$ and k_m, we obtain eq 12. Resemblance of the case of intercage quenching to the case of intracage quenching is obvious: the structure of the solution remains the same, and the only thing we need to do is redefine the rate constants and take care of the occupancy numbers.

Supporting Information Available: The experimental decay curves of ^{3}A* at various loading levels of the quenchers. This material is available free of charge via the Internet at http://pubs.acs.org.

References and Notes

(1) Kärger, J.; Ruthven, D. M. *Diffusion in Zeolites and Other Microporous Solids*; Wiley-Interscience: New York, 1992.

(2) Chen, N. Y.; Degnan, T. F.; Smith, C. M. *Molecular Transport and Reaction in Zeolites*; VCH: New York, 1994.

(3) Thomas, J. K. *Chem. Rev.* **1993**, *93*, 301.

(4) Ramamurthy, V.; Robbins, R. J.; Thomas, K. J.; Lakshiminarasimhan, P. H. In *Organized Molecular Assemblies in the Solid State*; Whitesell, J. K., Ed.; Wiley: Chichester, U.K., 1999; pp 63−140.

(5) (a) Burmeister, R.; Schwarz, H.; Boddenberg, B. *Ber. Bunsen-Ges. Phys. Chem.* **1989**, *93*, 1309. (b) Bull, L. M.; Henson, N. J.; Cheetham, A. K.; Newsam, J. M.; Heyes, S. J. *J. Phys. Chem.* **1993**, *97*, 11776. (c) Sousa Gonçalves, J. A.; Portsmouth, R. L.; Alexander, P.; Gladden, L. F. *J. Phys. Chem.* **1995**, *99*, 3317. (d) Auerbach, S. M.; Bull, L. M.; Henson, N. J.; Metiu, H. I.; Cheetham, A. K. *J. Phys. Chem.* **1996**, *100*, 5923.

(6) (a) Germanus, A.; Kärger, J.; Pfeifer, H.; Samulevic, Zd'anov, S. P. *Zeolites* **1985**, *5*, 91. (b) Kärger, J.; Pfeifer, H. *Zeolites* **1987**, *7*, 90.

(7) (a) Czjzek, M.; Jobic, H.; Bee, M. *J. Chem. Soc., Faraday Trans. 1* **1991**, *87*, 3455. (b) Jobic, H.; Fitch, A. N.; Combet, J. *J. Phys. Chem. B* **2000**, *104*, 8491.

(8) (a) Kärger, J.; Ruthven, D. M. *J. Chem. Soc., Faraday Trans. 1* **1981**, *77*, 1485. (b) Eic, M.; Goddard, M.; Ruthven, D. M. *Zeolites* **1988**, *8*, 327.

(9) Klein, H.; Fuess, H.; Schrimpf, G. *J. Phys. Chem.* **1996**, *100*, 11101.

(10) (a) Auerbach, S. M.; Metiu, H. I. *J. Chem. Phys.* **1996**, *105*, 3753. (b) Auerbach, S. M.; Metiu, H. I. *J. Chem. Phys.* **1997**, *106*, 2893.

(11) Fitch, A. N.; Jobic, H.; Renouprez, A. *J. Phys. Chem.* **1986**, *90*, 1311.

(12) (a) Chmelka, B. F.; Rafterry, D.; McCormick, A. V.; de Menorval, L. C.; Levine, R. D.; Pines, A. *Phys. Rev. Lett.* **1991**, *66*, 580. (b) Rarsen, R. G.; Shore, J.; Schmidt-Rohr, K.; Emsley, L.; Long, H.; Pines, A.; Janicke, M.; Chmelka, B. F. *Chem. Phys. Lett.* **1993**, *214*, 220.

(13) Post, M. F. M. *Stud. Surf. Sci. Catal.* **1991**, *58*, 391.

(14) Scaiano, J. C.; de Lucas, N. C.; Andraos, J.; García, H. *Chem. Phys. Lett.* **1995**, *233*, 5.
(15) Dexter, D. L. *J. Chem. Phys.* **1953**, *21*, 836.
(16) (a) Almgren, M. In *Kinetics and Catalysis in Microheterogeneous Systems*; Grätzel, M., Kalyanasundaram, K., Eds.; Marcel Dekker: New York, 1991; p 63. (b) Gehlen, M. H.; De Schryver, F. C. *Chem. Rev.* **1993**, *93*, 199.
(17) Barzykin, A. V.; Hashimoto, S. *J. Chem. Phys.* **2000**, *113*, 2841.
(18) Johnston, L. J.; Sciano, J. C.; Ji-Liang, S.; Siebrand, W.; Zerbetto, F. *J. Phys. Chem.* **1991**, *95*, 10018.
(19) (a) Kessler, R. W.; Krabichler, G.; Uhl, S.; Oelkrug, D.; Hagen, W.; Hyslop, J.; Wilkinson, F. *Opt. Acta* **1983**, *30*, 1099. (b) Wilkinson, F. *J. Chem. Soc., Faraday Trans. 2* **1986**, *82*, 2073. (c) Oelkrug, D.; Honnen, W.; Wilkinson, F.; Willsher, C. J. *J. Chem. Soc., Faraday Trans. 2* **1987**, *83*, 2081.
(20) (a) Dutta, P. K.; Thomson, M. A. *Chem. Phys. Lett*. **1986**, *131*, 435. (b) Overweg, A. R.; Koller, H.; Haan, J. W.; van de Ven, L. M.; van der Kraan, A. M.; van Santen, R. A. *J. Phys. Chem. B* **1999**, *103*, 4298.
(21) Weiss, G. H. *Aspects and Applications of the Random Walk*; North-Holland, Amsterdam, 1994.
(22) (a) Zumofen, G.; Blumen, A.; Klafter, J. *J. Chem. Phys.* **1985**, *82*, 3198. (b) Barzykin, A. V.; Tachiya, M. *Phys. Rev. Lett.* **1994**, *73*, 3479.
(23) (a) Infelta, P. P.; Grätzel, M.; Thomas, J. K. *J. Phys. Chem.* **1974**, *78*, 190. (b) Tachiya, M. *Chem. Phys. Lett.* **1975**, *33*, 289.
(24) Rice, S. A. *Diffusion-Limited Reactions*; Elsevier: Amsterdam, 1985.
(25) Benssason, R.; Land, E. J. *Trans. Faraday Soc*. **1971**, *67*, 1904.
(26) Saltiel, J.; Marchand, G. R.; Dabestani, R.; Pecha, M. *Chem. Phys. Lett*. **1983**, *100*, 219.
(27) (a) Buettner, A. V. *J. Phys. Chem*. **1964**, *68*, 3253. (b) Kellog, R. E. *J. Chem. Phys*. **1966**, *44*, 411. (c) Beckett, A. *Nature* **1966**, *211*, 410.
(28) The main reason the self-quenching is observed in NaY, despite low diffusivity, is because of sufficiently high concentration in the cage networks. For instance, a typically low loading of 5.0×10^{-6} mol g^{-1} corresponds to 1.3×10^{-2} mol dm^{-3} and a relatively high loading of 1.0×10^{-4} mol g^{-1} corresponds to 2.6×10^{-1} mol dm^{-3}.
(29) Murov, S. L.; Carmichael, I.; Hug, G. L. *Handbook of Photochemistry*, 2nd ed.; Marcel Dekker: New York, 1993; pp 56−98.
(30) Murov, S. L.; Carmichael, I.; Hug, G. L. *Handbook of Photochemistry*, 2nd ed.; Marcel Dekker: New York, 1993; p 226.
(31) The RC time constant of the detection system is ca. 100 ns, which may not be fast enough to measure the rate of intracage quenching. Besides, the sampling interval was set to 10 μs because of the necessity to cover the millisecond time scale.
(32) Hashimoto, S.; Miyashita, T.; Hagiri, M. *J. Phys. Chem. B* **1999**, *103*, 9149.
(33) Ellison, E. H. *J. Phys. Chem. B* **1999**, *103*, 9314.
(34) Lechert, H.; Basler, W. D. *J. Phys. Chem. Solids* **1989**, *50*, 497.
(35) Kärger, J.; Ruthven, D. M. *Diffusion in Zeolites and Other Microporous Solids*; Wiley-Interscience: New York, 1992; p 453.
(36) Favre, D. E.; Schaefer, D. J.; Auerbach, S. M.; Chmelka, B. F. *Phys. Rev. Lett*. **1998**, *81*, 5852.